2018 Annual American Control Conference (ACC)
June 27–29, 2018. Wisconsin Center, Milwaukee, USA

Straight-Line Contouring Control of Fully Actuated 3-D Bipedal Robotic Walking

Yan Gu, Bin Yao, and C. S. George Lee †

Abstract— **Satisfactory tracking of a planned path on the walking surface is an important requirement for bipedal robotic walking in many applications. In this paper, a model-based feedback control strategy is proposed for fully actuated three-dimensional (3-D) bipedal robots to realize exponential tracking of a straight-line contour on the walking surface as well as the desired periodic or aperiodic motion along the contour. First, the full-order dynamic model of bipedal robotic walking is presented. Second, a state feedback control law is synthesized based on input-output linearization with the output function designed as the tracking errors of a straight-line contour on the walking surface, the desired position trajectory along the contour, and the desired walking pattern. Sufficient conditions for the exponential stability of the hybrid time-varying closed-loop system are then established based on formal stability analysis. Finally, simulation results had validated the proposed contouring control strategy on a 3-D bipedal robot with nine revolute joints.**

I. Introduction

To accomplish various complex tasks such as delivery service, disaster response, and space exploration, it is necessary that a bipedal robot is capable of highly versatile walking, such as satisfactorily tracking a planned path on the walking surface as well as the desired periodic or aperiodic motion along the path. Due to its high versatility, the Zero-Moment-Point (ZMP) walking control framework has been widely used to enable such position tracking capabilities [1] [2].

Another extensively studied approach of bipedal walking control is the Hybrid-Zero-Dynamics (HZD) framework [3]–[5]. The HZD framework realizes stable periodic bipedal robotic walking based on full-order dynamic modeling, nonlinear control theories, and formal stability analysis. As compared with the ZMP framework, the HZD framework can formally guarantee the closed-loop stability of the walking control system and achieve higher walking speed and energy efficiency. Because of these advantages, the HZD framework has enabled successful underactuated walking [6]–[9], fully actuated walking [10]–[12], 3-D walking [7] [13] [14], uneven terrain walking [15] [16], and running [17] [18]. However, because the HZD framework mainly addresses periodic walking, its versatility is not as high as the ZMP framework. Previous work on improving the walking versatility of the HZD framework includes extending the HZD framework to aperiodic gaits for underactuated walking [19] and realizing velocity tracking in Cartesian space for fully actuated walking [10]. Still, position tracking in Cartesian space and aperiodic walking stabilization have not been fully explored under the HZD framework.

In our previous studies, we have investigated time-dependent orbital stabilization for underactuated bipedal robotic walking through model-based feedback control [20]. However, the time-dependent orbital stabilization strategy cannot be used to achieve satisfactory position tracking in Cartesian space, which generally requires aperiodic walking stabilization for the purpose of high versatility. Therefore, we have proposed another model-based controller design to enable exponential position tracking in Cartesian space for fully actuated planar bipeds [21] [22]. To our best knowledge, it is the first time that position tracking in Cartesian space has been addressed for bipedal robotic walking through model-based feedback control and formal stability analysis. Still, this previous work on planar walking cannot be directly applied to 3-D walking.

The main objective of this study is to develop a state feedback controller that realizes exponential tracking of the desired position trajectory in Cartesian space. The problem of position tracking in Cartesian space will be formulated as a contouring control problem, which has been extensively studied for machining tasks such as cutting and milling [23] [24] but not for robotic locomotion. Here, we adapt the concept of contouring control from machining to bipedal robotic walking. A contour is defined as a 1-D geometric path on the walking surface, and the contouring control problem will be decomposed into two subproblems. One is a stabilization problem, and the objective is to realize exponential convergence to the shape of the desired contour. The other is a position tracking problem, and the objective is to realize exponential convergence to the desired periodic or aperiodic motion along the desired contour. As the initial step of our ongoing research, this study focuses on straight-line paths/contours.

This paper is structured as follows. Section II presents the full-order dynamic model of bipedal robotic walking. The proposed time-dependent output function design is introduced in Section III, and the input-output linearizing controller design is explained in Section IV. In Section V, sufficient closed-loop stability conditions are established. Simulation results on 3-D bipedal robotic walking are given in Section VI.

†Yan Gu is with the Department of Mechanical Engineering, University of Massachusetts Lowell, Lowell, MA 01854, U.S.A. Bin Yao is with the School of Mechanical Engineering, and C. S. George Lee is with the School of Electrical and Computer Engineering, Purdue University, West Lafayette, IN 47907, U.S.A. Email: yan_gu@uml.edu; {byao, csglee}@purdue.edu. Bin Yao, the corresponding author, is also a Chang-Jiang Chair Professor at Zhejiang University, China.

This work was supported in part by the National Science Foundation under Grant IIS-0916807. Any opinion, findings, and conclusions or recommendations expressed in this material are those of the authors and do not necessarily reflect the views of the National Science Foundation.

978-1-5386-5428-6/$31.00 ©2018 AACC

II. Hybrid Walking Dynamics

The main objective of this study is to achieve exponential position tracking in Cartesian space for fully actuated 3-D bipedal robotic walking through model-based feedback control. With this goal in mind, we first present the full-order model of bipedal walking dynamics.

A 3-D bipedal robot [13] is shown in Fig. 1. The world coordinate frame is fixed on the walking surface and denoted as $O_wX_wY_wZ_w$. Assume that the walking surface is flat and horizontal, that the biped has identical legs and massless thin feet, and that the swing ankle is not actuated [13]. Also, assume that the double-support phase when both feet touch the ground is instantaneous, that the swing-foot landing impact is modeled as a contact between rigid bodies, and, without loss of generality, that the swing foot always lands flat pointing towards the positive direction of the X_w-axis.

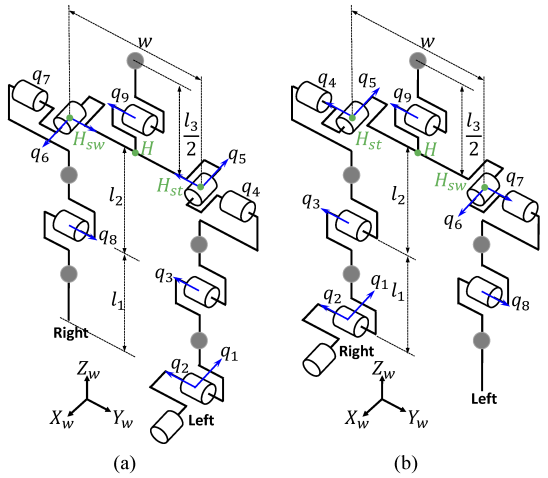

Fig. 1. A 3-D biped with the mass of each link lumped at the center. (a): Left leg is in support. (b): Right leg is in support. (l_1, l_2, and l_3 are lengths of lower limb, upper limb, and trunk, respectively, and w is the hip width.)

Under these assumptions, a complete step consists of a continuous single-support phase and a discrete landing impact. Let $Q \subset \mathbb{R}^9$ denote the configuration space of the robot when its support foot remains full, static contact with the walking surface and the joint position limits are satisfied (e.g., the knee joints cannot be bent forward). Let $\mathbf{q} = \left[q_1, q_2, q_3, q_4, q_5, q_6, q_7, q_8, q_9\right]^T \in Q$ and $\mathbf{u} = \left[u_1, u_2, u_3, u_4, u_5, u_6, u_7, u_8, u_9\right]^T \in \mathbb{R}^9$ denote the joint positions and torques, respectively. Definitions of q_i and u_i ($i = 1, 2, ..., 9$) are illustrated in Fig. 1. Because there are nine degrees of freedom during a continuous phase and nine independent actuators, the biped is fully actuated.

When the left leg is in support, the full-order model of walking dynamics during a continuous phase can be written as [3] [13]

$$\mathbf{M}_L(\mathbf{q})\ddot{\mathbf{q}} + \mathbf{c}_L(\mathbf{q}, \dot{\mathbf{q}}) = \mathbf{B}_u\mathbf{u}, \tag{1}$$

where $\mathbf{M}_L$ is the inertia matrix, $\mathbf{c}_L$ is the sum of Coriolis, centrifugal, and gravitational terms, and $\mathbf{B}_u$ is the input matrix. When the right leg is in support, the inertia matrix $\mathbf{M}_R$ and the vector $\mathbf{c}_R$ can be obtained by replacing w with $-w$ in the expressions of $\mathbf{M}_L$ and $\mathbf{c}_L$, respectively [13].

When the swing leg hits the walking surface, an impact occurs. The variable $\mathbf{q}$ will experience a sudden jump because of the coordinate swap. The variable $\dot{\mathbf{q}}$ will also be discontinuous because of the coordinate swap and the rigid-body impact. The reset map from the left-in-support to the right-in-support phase can be expressed as [3] [13]

$$\left[\mathbf{q}^+; \dot{\mathbf{q}}^+\right] = \left[\mathbf{\Delta}_{qL}(\mathbf{q}^-); \mathbf{\Delta}_{\dot{q}L}(\mathbf{q}^-)\dot{\mathbf{q}}^-\right] := \mathbf{\Delta}_L(\mathbf{q}^-, \dot{\mathbf{q}}^-). \tag{2}$$

The right-to-left-in-support reset map, denoted as $\mathbf{\Delta}_R$, can be obtained by replacing w with $-w$ in $\mathbf{\Delta}_L$.

The moment of a swing-foot landing is determined by the switching surface $S_q(\mathbf{q}, \dot{\mathbf{q}})$:

$$S_q(\mathbf{q}, \dot{\mathbf{q}}) := \{(\mathbf{q}, \dot{\mathbf{q}}) \in TQ : z_{sw}(\mathbf{q}) = 0,\ \dot{z}_{sw}(\mathbf{q}, \dot{\mathbf{q}}) < 0\}, \tag{3}$$

where z_{sw} is the swing foot height.

The overall hybrid system dynamics can be expressed as:

$$\begin{cases} \Sigma_L : \begin{cases} \mathbf{M}_L(\mathbf{q})\ddot{\mathbf{q}} + \mathbf{c}_L(\mathbf{q}, \dot{\mathbf{q}}) = \mathbf{B}_u\mathbf{u}, & \text{if } (\mathbf{q}^-, \dot{\mathbf{q}}^-) \notin S_L(\mathbf{q}, \dot{\mathbf{q}}); \\ [\mathbf{q}^+; \dot{\mathbf{q}}^+] = \mathbf{\Delta}_L(\mathbf{q}^-, \dot{\mathbf{q}}^-), & \text{if } (\mathbf{q}^-, \dot{\mathbf{q}}^-) \in S_L(\mathbf{q}, \dot{\mathbf{q}}); \end{cases} \\ \Sigma_R : \begin{cases} \mathbf{M}_R(\mathbf{q})\ddot{\mathbf{q}} + \mathbf{c}_R(\mathbf{q}, \dot{\mathbf{q}}) = \mathbf{B}_u\mathbf{u}, & \text{if } (\mathbf{q}^-, \dot{\mathbf{q}}^-) \notin S_R(\mathbf{q}, \dot{\mathbf{q}}); \\ [\mathbf{q}^+; \dot{\mathbf{q}}^+] = \mathbf{\Delta}_R(\mathbf{q}^-, \dot{\mathbf{q}}^-), & \text{if } (\mathbf{q}^-, \dot{\mathbf{q}}^-) \in S_R(\mathbf{q}, \dot{\mathbf{q}}); \end{cases} \end{cases} \tag{4}$$

where the switching surfaces $S_L(\mathbf{q}, \dot{\mathbf{q}})$ and $S_R(\mathbf{q}, \dot{\mathbf{q}})$ can be obtained from $S_q(\mathbf{q}, \dot{\mathbf{q}})$ with the corresponding expressions of the swing foot height $z_{sw}(\mathbf{q})$.

III. Time-dependent Output Function Design

To realize exponential tracking of the desired contour and the desired motion along the contour on the walking surface, the associated tracking errors will be used for output function design, and input-output linearization will be utilized to synthesize a feedback controller that exponentially drives the output function to zero. In this section, the proposed time-dependent output function design will be introduced.

Since the robot has nine independent actuators, nine independent output functions can be designed. Two of them will be chosen as the contour tracking error and the position tracking error along the planned contour. The other seven output functions will be designed as the tracking error of the desired walking pattern such that the variables of interest (e.g., the trunk angle and the swing foot position) can be directly controlled with respect to a phase variable that represents how far a step has progressed.

1) Contour and Position Tracking Error: Let Γ_d be the desired contour on the walking surface. An orthogonal coordinate frame can be established along the desired contour [24]: the curvilinear coordinate r_c along the normal direction of the desired contour represents the contouring error, and the curvilinear coordinate r_m represents the position along the desired contour. As the first step of our ongoing investigation, the desired contour Γ_d is chosen as a straight line on the walking surface, which, for simplicity and without loss of generality, is chosen as the X_w-axis, i.e.,

$$\Gamma_d = \{(x_h, y_h) \in \mathbb{R}^2 : y_h = 0\}, \tag{5}$$

where (x_h, y_h) is the horizontal hip position with respect to (w.r.t.) the world coordinate frame and is chosen to represent a biped's global position in Cartesian space. Then, one has

$$r_c = y_h \text{ and } r_m = x_h. \tag{6}$$

Let $s_d(t)$ be the desired position trajectory along the desired contour Γ_d. In this study, $s_d(t)$ is defined as monotonically increasing and continuously differentiable in t. For the purpose of high walking versatility, the velocity profile of $s_d(t)$ can be periodic or aperiodic.

From Eqs. (5) and (6), it is clear that the contour tracking error is y_h, and the position tracking error along the desired contour is $x_h - s_d(t)$. Thus, the objectives of contouring control are: 1) to drive y_h to zero; 2) to drive x_h to $s_d(t)$.

2) Walking Pattern Tracking Error: A walking pattern represents the relative evolution of configuration-based variables with respect to a phase variable [3]. Denote the desired walking pattern as

$$\mathbf{h}_c(\mathbf{q}) - \boldsymbol{\phi}(\theta(\mathbf{q})) = \mathbf{0}, \tag{7}$$

where $\theta : Q \to Q_f \subset \mathbb{R}$ is a phase variable, which is monotonically increasing during a step and represents how far a step has progressed, $\mathbf{h}_c : Q \to Q_c \subset \mathbb{R}^7$ is a set of configuration-based variables that are of interest to be controlled and is continuously differentiable in $\mathbf{q} \in Q$, and $\boldsymbol{\phi}(\theta) : Q_f \to \mathbb{R}^7$ is the desired trajectory of $\mathbf{h}_c(\mathbf{q})$ and is continuously differentiable in $\theta \in Q_f$.

From (7), it is clear that the tracking error of the desired walking pattern is $\mathbf{h}_c(\mathbf{q}) - \boldsymbol{\phi}(\theta(\mathbf{q}))$.

Here, $\mathbf{h}_c(\mathbf{q})$ is designed as

$$\mathbf{h}_c(\mathbf{q}) := \left[q_9, \theta_{r,h}(\mathbf{q}), \theta_{p,h}(\mathbf{q}), x_{h2sw}(\mathbf{q}), y_{h2sw}(\mathbf{q}), z_{sw}(\mathbf{q}), z_h(\mathbf{q})\right], \tag{8}$$

where the trunk joint angle q_9 and the swing foot height z_{sw} are already defined and the rest of the elements are defined w.r.t. the world coordinate frame as follows:

- $\theta_{r,h}(\mathbf{q})$ is the angle from the horizontal plane to the vector $\overrightarrow{H_{st}H_{sw}}$ where H_{st} and H_{sw} represent the hip joints of the support and the swing legs, respectively (see Fig. 1);
- $\theta_{p,h}(\mathbf{q})$ is the angle from the Z_w-axis to the trunk link;
- ($x_{h2sw}(\mathbf{q})$,$y_{h2sw}(\mathbf{q})$) is the swing foot's horizontal relative position w.r.t. the pelvis H;
- $z_h(\mathbf{q})$ is the height of the pelvis H above the walking surface.

The desired trajectory $\boldsymbol{\phi}(\theta)$ is encoded by the phase variable θ and is designed as $\boldsymbol{\phi} := [\phi_1, \phi_2, \phi_3, \phi_4, \phi_5, \phi_6, \phi_7]^T$. As forward walking along the X_w-axis is of interest in this study, the hip's relative position w.r.t. the support foot along the X_w-axis will be chosen as the phase variable. Letting $\bar{x}_h : Q \to Q_x \subset \mathbb{R}$ and $\bar{y}_h : Q \to Q_y \subset \mathbb{R}$ be the x- and y-coordinates of the hip's relative position with respect to the support foot, respectively, one has $\theta := \bar{x}_h(\mathbf{q})$. Similar to the HZD framework [4] and our previous work [20]–[22], Bezier curves are used to parameterize the desired function $\boldsymbol{\phi}(\theta)$ as

$$\boldsymbol{\phi}(\theta) := \sum_{k=0}^{M} \mathbf{a}_k \frac{M!}{k!(M-k)!} s(\theta)^k (1 - s(\theta))^{M-k}, \tag{9}$$

where $s(\theta) := \frac{\theta - \theta_0}{\theta^* - \theta_0}$, θ_0 and θ^* are the planned values of θ at the beginning and the end of a step, respectively, and $\mathbf{a}_k \in \mathbb{R}^7$ is the unknown vector to be optimized in Section VI. For simplicity, only symmetric gaits are discussed in this study. Therefore, the desired function $\boldsymbol{\phi}(\theta)$ is the same for both the left-in-support and the right-in-support phases except for the function $\phi_5(\theta)$ because it defines the desired trajectory of y_{h2sw}. Define $\phi_5(\theta)$ as

$$\phi_5(\theta) := \begin{cases} \phi_{5L}(\theta), & \text{(left-in-support);} \\ \phi_{5R}(\theta), & \text{(right-in-support).} \end{cases} \tag{10}$$

Because of the left-right symmetry, $\phi_{5L}(\theta) = -\phi_{5R}(\theta)$. Hence, $\boldsymbol{\phi}(\theta)$ can be completely determined by considering either the left- or the right-in-support phase.

3) Output Function Design: We are now ready to introduce the following output function design:

$$\mathbf{y} = \mathbf{h}(t, \mathbf{q}) := \begin{bmatrix} x_h - s_d(t) \\ y_h \\ \mathbf{h}_c(\mathbf{q}) - \boldsymbol{\phi}(\theta) \end{bmatrix} = \begin{bmatrix} \bar{x}_h(\mathbf{q}) \\ \bar{y}_h(\mathbf{q}) \\ \mathbf{h}_c(\mathbf{q}) \end{bmatrix} - \begin{bmatrix} -x_{st,k-1} + s_d(t) \\ -y_{st,k-1} \\ \boldsymbol{\phi}(\theta) \end{bmatrix}, \tag{11}$$

where $(x_{st,k-1}, y_{st,k-1})$ is the stance foot horizontal position w.r.t. the world coordinate frame during the k^{th} ($k \in \{1, 2, ...\}$) actual step.

If the output function $\mathbf{y}$ is exponentailly driven to zero through input-output linearizing control, then exponential tracking of the desired contour, the desired motion along the contour, and the desired walking pattern will be realized.

Remark: With the proposed design of $\mathbf{h}_c(\mathbf{q})$ in Eq. (8), it can be proved that there exists a diffeomorphism $D : Q_x \times Q_y \times Q_c \to Q$ when $q_9 = 0$ (i.e., the joint angle of trunk is 0), $\theta_{r,h}(\mathbf{q}) = 0$ (i.e., the hip link is horizontal), and $\theta_{p,h}(\mathbf{q}) = 0$ (i.e., the trunk link is upright).

IV. Model-based Feedback Control through Input-Output Linearization

To drive the output function to zero, a state feedback controller is designed through input-output linearization [25].

During a continuous phase, the feedback control law is chosen as

$$\mathbf{u} = \mathbf{u}_i = (\tfrac{\partial \mathbf{h}}{\partial \mathbf{q}} \mathbf{M}_i^{-1} \mathbf{B})^{-1} (\mathbf{v} + \tfrac{\partial \mathbf{h}}{\partial \mathbf{q}} \mathbf{M}_i^{-1} \mathbf{c}_i - \tfrac{\partial^2 \mathbf{h}}{\partial t^2} - \tfrac{\partial}{\partial \mathbf{q}} (\tfrac{\partial \mathbf{h}}{\partial \mathbf{q}} \dot{\mathbf{q}}) \dot{\mathbf{q}}) \tag{12}$$

where the index $i \in \{L, R\}$ indicates whether the left (L) or the right (R) leg is in support.

The continuous-phase dynamics then become $\ddot{\mathbf{y}} = \mathbf{v}$. Choosing $\mathbf{v}$ as the proportional-derivative (PD) control law $\mathbf{v} = -\mathbf{K}_P \mathbf{y} - \mathbf{K}_D \dot{\mathbf{y}}$, where $\mathbf{K}_P \in \mathbb{R}^{9\times 9}$ and $\mathbf{K}_D \in \mathbb{R}^{9\times 9}$ are positive-definite diagonal matrices, one then obtains the following linear dynamics:

$$\begin{bmatrix} \dot{\mathbf{y}} \\ \ddot{\mathbf{y}} \end{bmatrix} = \begin{bmatrix} \mathbf{0} & \mathbf{I} \\ -\mathbf{K}_P & -\mathbf{K}_D \end{bmatrix} \begin{bmatrix} \mathbf{y} \\ \dot{\mathbf{y}} \end{bmatrix} := \mathbf{A} \begin{bmatrix} \mathbf{y} \\ \dot{\mathbf{y}} \end{bmatrix}, \tag{13}$$

where $\mathbf{0} \in \mathbb{R}^{9\times 9}$ is a zero matrix and $\mathbf{I} \in \mathbb{R}^{9\times 9}$ is an identity matrix.

Defining $\mathbf{x} := \left[\mathbf{y}; \dot{\mathbf{y}}\right] \in \mathbb{R}^{18}$, one can compactly rewrite the closed-loop dynamics as:

$$\begin{cases} \Sigma_L : \begin{cases} \dot{\mathbf{x}} = \mathbf{A}\mathbf{x}, & \text{if } (t, \mathbf{x}^-) \notin S_{L\to R}(t, \mathbf{x}); \\ \mathbf{x}^+ = \boldsymbol{\Delta}_{L\to R}(t, \mathbf{x}^-), & \text{if } (t, \mathbf{x}^-) \in S_{L\to R}(t, \mathbf{x}); \end{cases} \\ \Sigma_R : \begin{cases} \dot{\mathbf{x}} = \mathbf{A}\mathbf{x}, & \text{if } (t, \mathbf{x}^-) \notin S_{R\to L}(t, \mathbf{x}); \\ \mathbf{x}^+ = \boldsymbol{\Delta}_{R\to L}(t, \mathbf{x}^-), & \text{if } (t, \mathbf{x}^-) \in S_{R\to L}(t, \mathbf{x}); \end{cases} \end{cases} \tag{14}$$

where the expressions of $\boldsymbol{\Delta}_{L\to R}$, $\boldsymbol{\Delta}_{R\to L}$, $S_{L\to R}$, and $S_{R\to L}$ can be obtained from Eqs. (2), (3), and (11). Note that $\boldsymbol{\Delta}_{L\to R}$, $\boldsymbol{\Delta}_{R\to L}$, $S_{L\to R}$, and $S_{R\to L}$ are time-dependent because the proposed output function design in Eq. (11) is time-dependent.

If $\mathbf{K}_P$ and $\mathbf{K}_D$ are chosen such that $\mathbf{A}$ is Hurwitz, then there exists a real positive-definite-symmetric matrix $\mathbf{W}$ such that $V(\mathbf{x}) = \mathbf{x}^T\mathbf{W}\mathbf{x}$ is a Lyapunov function candidate for the continuous-phase dynamics. Also, there exist positive constants c_1, c_2, and c_3 such that $V(\mathbf{x})$ satisfies

$$c_1\|\mathbf{x}\|^2 \leq V(\mathbf{x}) \leq c_2\|\mathbf{x}\|^2 \text{ and } \dot{V}(\mathbf{x}) \leq -c_3 V(\mathbf{x}) \tag{15}$$

for all $\mathbf{x}$ during each continuous phase [25].

V. Closed-loop Stability Analysis

In this section, the closed-loop stability of the hybrid time-varying system in Eq. (14) is analyzed. Before introducing the main theorem on closed-loop stability, we first present some properties of the system.

Suppose that the walking process begins with the left-in-support continuous phase. The k^{th} ($k \in \{1,2,...\}$) switching surface S_k is defined as

$$S_k(t,\mathbf{x}) := \begin{cases} S_{L\to R}(t,\mathbf{x}), & \text{if } k \in \{1,3,5,...\}; \\ S_{R\to L}(t,\mathbf{x}), & \text{if } k \in \{2,4,6,...\}. \end{cases}$$

Let T_{k-1} be the initial moment of the k^{th} ($k \in \{1,2,...\}$) actual step. Without loss of generality, define $T_0 = 0$. Then, T_k represents the moment of the first intersection with the k^{th} switching surface $S_k(t,\mathbf{x})$ on $t > T_{k-1}^+$, i.e., the moment of the k^{th} actual swing-foot touchdown. In the following, $\star(T_{k-1}^-)$ and $\star(T_{k-1}^+)$ will be denoted as $\star|_{k-1}^-$ and $\star|_{k-1}^+$, respectively.

Let τ_k be the k^{th} ($k \in \{1,2,...\}$) desired touchdown moment. Then, τ_k represents the moment of the first intersection with the k^{th} switching surface $S_k(t,\mathbf{x})$ on $t > T_{k-1}^+$ assumsing $\mathbf{x} = \mathbf{0}$ $\forall t > T_{k-1}^+$.

Theorem 1 (Fixed Value of θ at the Desired Impact) With properly designed $\boldsymbol{\phi}(\theta)$ and under the assumption that $\mathbf{x} = \mathbf{0}$ $\forall t > T_{k-1}^+$, there exists a constant θ^* such that $\theta(\tau_k^-) = \theta^*$ holds $\forall k \in \{1,2,...\}$. ■

Sketch of Proof: By the definitions of τ_k, S_k, and $\mathbf{y}$, and under the assumption that $\mathbf{x} = \mathbf{0}$ $\forall t > T_{k-1}^+$, one has $z_{sw}(\tau_k^-) = 0$ and $z_{sw}(\tau_k^-) = \phi_6(\theta)$. Thus, $\phi_6(\theta(\tau_k^-)) = 0$ holds, which, along with the fact that θ increases monotonically during a step, indicates that there exists a constant θ^* such that $\theta(\tau_k^-) = \theta^*$ holds $\forall k \in \{1,2,...\}$ if $\boldsymbol{\phi}(\theta)$ is properly designed [4]. ■

To guarantee the fixed value of θ at the desired impact, a proper design of $\boldsymbol{\phi}(\theta)$ should guarantee a unique solution of

$$\left[\bar{x}_h(\mathbf{q}); \bar{y}_h(\mathbf{q}); \mathbf{h}_c(\mathbf{q})\right] = \left[\theta^*; -y_{st,k-1}; \boldsymbol{\phi}(\theta^*)\right] \tag{16}$$

for $\mathbf{q} \in Q$ [4]. Recall that a diffeomorphism $D : Q_x \times Q_y \times Q_c \to Q$ exists when $q_9, \theta_{r,h}(\mathbf{q}), \theta_{p,h}(\mathbf{q}) = 0$. Thus, the solution uniqueness can be guaranteed with $\phi_1(\theta), \phi_2(\theta), \phi_3(\theta) = 0$. Other requirements for a proper design of $\boldsymbol{\phi}(\theta)$ are summarized in Theorem 2.

Theorem 2 (Hybrid Invariance under the Condition $y_{st,k-1} = y_{std}$) Denote $\mathbf{H}_v(\mathbf{q}) := [\frac{d\bar{x}_h}{d\mathbf{q}}(\mathbf{q}); \frac{d\bar{y}_h}{d\mathbf{q}}(\mathbf{q}); \frac{d\mathbf{h}_c}{d\mathbf{q}}(\mathbf{q})]$. Let the desired function $\boldsymbol{\phi}(\theta)$ satisfy the following conditions:

(A1) $\mathbf{h}_c(\boldsymbol{\Delta}_q(\mathbf{q}^*)) = \boldsymbol{\phi}(\bar{x}_h(\boldsymbol{\Delta}_q(\mathbf{q}^*)))$;

(A2) $\frac{d\bar{x}_h}{d\mathbf{q}}(\boldsymbol{\Delta}_q(\mathbf{q}^*))\boldsymbol{\Delta}_{\dot{q}}(\mathbf{q}^*)\mathbf{H}_v^{-1}(\mathbf{q}^*)\left[1;0;\frac{d\boldsymbol{\phi}}{d\theta}(\theta^*)\right] = 1$;

(A3) $\mathbf{H}_v(\boldsymbol{\Delta}_q(\mathbf{q}^*))\boldsymbol{\Delta}_{\dot{q}}(\mathbf{q}^*)\mathbf{H}_v^{-1}(\mathbf{q}^*)\left[1;0;\frac{d\boldsymbol{\phi}}{d\theta}(\theta^*)\right]$
$= \left[1;0;\frac{d\boldsymbol{\phi}}{d\theta}(\bar{x}_h(\boldsymbol{\Delta}_q(\mathbf{q}^*)))\right]$;

where $\mathbf{q}^*$ is a solution of Eq. (16) with $y_{st,k-1} = y_{std} := \phi_5(\theta^*)$ for $\mathbf{q} \in Q$. Then, hybrid invariance (i.e., if $\mathbf{x}(\tau_k^-) = \mathbf{0}$, then $\mathbf{x}(\tau_k^+) = \mathbf{0}$) holds under $y_{st,k-1} = y_{std} := \phi_5(\theta^*)$. ■

The proof of Theorem 2 can be constructed as an extension of our previous study on planar walking [21] [22], which is omitted due to space limitations.

Remark: Although the restrictive condition $y_{st,k-1} = y_{std}$ is required for the hybrid invariance construction in Theorem 2, it is not required for the establishment of the closed-loop stability conditions in Theorem 3.

Theorem 3 (Closed-Loop Stability Conditions) Let the conditions (A1)–(A3) in Theorem 2 hold. The closed-loop control system in Eq. (14) is locally exponentially stable if the PD gains are chosen such that $\mathbf{A}$ in Eq. (14) is Hurwitz and that the continuous-phase convergence rate of the output function $\mathbf{y}$ is sufficiently fast. ■

Sketch of Proof: Let $V(\mathbf{x})$ be the Lyapunov function candidate. By stability analysis based on the construction of multiple Lyapunov functions [26], the hybrid time-varying system in Eq. (14) is locally exponentially stable if there exists a positive number d such that $V(\mathbf{x})$ is exponentially decreasing during each continuous phase and that $\{V|_1^+, V|_2^+, V|_3^+, ...\}$ is a strictly decreasing sequence for any $\mathbf{x}(0^+) \in B_d(\mathbf{0}) := \{\mathbf{x} \in \mathbb{R}^{18} : \|\mathbf{x}\| \leq d\}$.

If the PD gains $\mathbf{K}_P$ and $\mathbf{K}_D$ are chosen such that the matrix $\mathbf{A}$ in Eq. (14) is Hurwitz, then, from Eq. (15), one has

$$V|_k^- \leq e^{-c_3(T_{k+1}-T_k)}V|_{k-1}^+ \tag{17}$$

during the k^{th} ($k \in \{1,2,...\}$) step, i.e., $V(\mathbf{x})$ is exponentially decreasing during each continuous phase.

Next, the convergence of the sequence $\{V|_1^+, V|_2^+, V|_3^+, ...\}$ will be analyzed.

At the k^{th} ($k \in \{1,2,...\}$) impact event, the corresponding k^{th} reset map $\boldsymbol{\Delta}_k$ is defined as

$$\boldsymbol{\Delta}_k(t,\mathbf{x}) := \begin{cases} \boldsymbol{\Delta}_{L\to R}(t,\mathbf{x}), & \text{if } k \in \{1,3,5,...\}; \\ \boldsymbol{\Delta}_{R\to L}(t,\mathbf{x}), & \text{if } k \in \{2,4,6,...\}. \end{cases}$$

To explicitly discuss the effect of $y_{st,k-1}$ on the reset map of $\mathbf{y}$ and $\dot{\mathbf{y}}$ at the k^{th} actual impact moment T_k, the reset map is rewritten as $\boldsymbol{\Delta}_k(T_k^-, \mathbf{x}|_k^-) = \boldsymbol{\Delta}_k(T_k^-, \mathbf{x}|_k^-, y_{st,k-1})$.

Because $\mathbf{x}|_k^+ = \boldsymbol{\Delta}_k(T_k^-, \mathbf{x}|_k^-)$, one has

$$\begin{aligned} &\|\mathbf{x}|_k^+\| = \|\boldsymbol{\Delta}_k(T_k^-, \mathbf{x}|_k^-, y_{st,k-1})\| \\ \leq &\|\boldsymbol{\Delta}_k(T_k^-, \mathbf{x}|_k^-, y_{st,k-1}) - \boldsymbol{\Delta}_k(\tau_k^-, \mathbf{x}|_k^-, y_{st,k-1})\| \\ &+ \|\boldsymbol{\Delta}_k(\tau_k^-, \mathbf{x}|_k^-, y_{st,k-1}) - \boldsymbol{\Delta}_k(\tau_k^-, \mathbf{0}, y_{st,k-1})\| \\ &+ \|\boldsymbol{\Delta}_k(\tau_k^-, \mathbf{0}, y_{st,k-1}) - \boldsymbol{\Delta}_k(\tau_k^-, \mathbf{0}, y_{std})\| + \|\boldsymbol{\Delta}_k(\tau_k^-, \mathbf{0}, y_{std})\|. \end{aligned} \tag{18}$$

As the desired function $\boldsymbol{\phi}(\theta)$ satisfies the conditions (A1)–(A3) in Theorem 2, one has

$$\|\boldsymbol{\Delta}_k(\tau_k^-, \mathbf{0}, y_{std})\| = \mathbf{0}. \tag{19}$$

Because the reset map $\boldsymbol{\Delta}_k(t, \mathbf{x}, y_{st,k-1})$ is continuously differentiable in t, $\mathbf{x}$, and $y_{st,k-1}$, there exists a positive constant r_1 and Lipschitz constants L_{Δ_t}, L_{Δ_x}, and $L_{\Delta_{st}}$ such that the following inequalities hold for any $\mathbf{x}(0^+) \in B_{r_1}(\mathbf{0})$:

$$\begin{aligned} &\|\boldsymbol{\Delta}_k(T_k^-, \mathbf{x}|_k^-, y_{st,k-1}) - \boldsymbol{\Delta}_k(\tau_k^-, \mathbf{x}|_k^-, y_{st,k-1})\| \leq L_{\Delta_t}|T_k - \tau_k|, \\ &\|\boldsymbol{\Delta}_k(\tau_k^-, \mathbf{x}|_k^-, y_{st,k-1}) - \boldsymbol{\Delta}_k(\tau_k^-, \mathbf{0}, y_{st,k-1})\| \leq L_{\Delta_x}\|\mathbf{x}|_k^-\|, \\ &\|\boldsymbol{\Delta}_k(\tau_k^-, \mathbf{0}, y_{st,k-1}) - \boldsymbol{\Delta}_k(\tau_k^-, \mathbf{0}, y_{std})\| \leq L_{\Delta_{st}}|y_{st,k-1} - y_{std}|. \end{aligned} \tag{20}$$

By [Theorem 1, [22]], there exists a positive constant r_2

and a Lipschitz constant L_{T_x} such that

$$|T_k - \tau_k| \le L_{T_x} \|\tilde{\mathbf{x}}(\tau_k; T_{k-1}^+, \mathbf{x}|_{k-1}^+)\| \tag{21}$$

for any $\mathbf{x}(0^+) \in B_{r_2}(\mathbf{0})$, where $\tilde{\mathbf{x}}(t; t_0, \lambda_0)$ denotes a solution of $\dot{\tilde{\mathbf{x}}} = \mathbf{A}\tilde{\mathbf{x}}$ with the initial condition $\tilde{\mathbf{x}}(t_0) = \lambda_0$, $\forall t > t_0$. Then, from Eqs. (20) and (21), one has

$$\begin{aligned} &\|\boldsymbol{\Delta}_k(T_k^-, \mathbf{x}|_k^-, y_{st,k-1}) - \boldsymbol{\Delta}_k(\tau_k^-, \mathbf{x}|_k^-, y_{st,k-1})\| \\ &\le L_{\Delta_t} L_{T_x} \|\tilde{\mathbf{x}}(\tau_k; T_{k-1}^+, \mathbf{x}|_{k-1}^+)\| \end{aligned} \tag{22}$$

for any $\mathbf{x}(0^+) \in B_{d_1}(\mathbf{0})$, where $d_1 = \min\{r_1, r_2\}$.

From Eqs. (20) and (21), one can also prove that there exist positive constants d_2 and β_{st} such that

$$\begin{aligned} &\|\boldsymbol{\Delta}_k(\tau_k^-, \mathbf{0}, y_{st,k-1}) - \boldsymbol{\Delta}_k(\tau_k^-, \mathbf{0}, y_{std})\| \\ &\le L_{\Delta_{st}}(\|\mathbf{x}|_k^-\| + \beta_{st}\|\tilde{\mathbf{x}}(\tau_k; T_{k-1}^+, \mathbf{x}|_{k-1}^-)\|) \end{aligned} \tag{23}$$

holds $\forall \mathbf{x}(0^+) \in B_{d_2}(\mathbf{0})$. Note that $|y_{st,k-1} - y_{st,d}|$ is bounded because the lateral support foot position is indirectly controlled through the control of the lateral swing foot position. For space consideration, the proof of Eq. (23) is omitted.

From Eqs. (18)–(23), one has, for any $\mathbf{x}(0^+) \in B_{d_3}(\mathbf{0})$,

$$\|\mathbf{x}|_k^+\|^2 \le \tilde{L}(\|\tilde{\mathbf{x}}(\tau_k; T_{k-1}^+, \mathbf{x}|_{k-1}^-)\|^2 + \|\mathbf{x}|_k^-\|^2), \tag{24}$$

where $\tilde{L} := \max(2(L_{\Delta_t} L_{T_x} + L_{\Delta_{st}} \beta_{st})^2, 2(L_{\Delta_x} + L_{\Delta_{st}})^2)$ and $d_3 := \min\{d_1, d_2\}$.

From Eq. (15), one has

$$V(\tilde{\mathbf{x}}(\tau_k; T_{k-1}^+, \mathbf{x}|_{k-1}^-)) \le e^{-c_3(\tau_k - T_{k-1})} V|_{k-1}^+. \tag{25}$$

Therefore, from Eqs. (15), (17), (24), and (25), one has

$$V|_k^+ \le \tilde{L}\frac{c_2}{c_1}(1 + e^{-c_3(T_k - \tau_k)}) e^{-c_3 \Delta\tau_k} V|_{k-1}^+, \tag{26}$$

where $\Delta\tau_k := \tau_k - T_{k-1}$.

It can be proved that for any $\varepsilon > 0$ there exists a positive constant d_4 and PD gains $\mathbf{K}_P$ and $\mathbf{K}_D$ that coorespond to sufficiently high continuous-phase convergence rate c_3 such that

$$e^{-c_3(T_k - \tau_k)} \le 1 + \varepsilon \tag{27}$$

hold for any $\mathbf{x}(0^+) \in B_{d_4}(\mathbf{0})$.

Hence, from Eqs. (26) and (27), one has

$$V|_k^+ \le \tilde{L}\frac{c_2}{c_1}(2 + \varepsilon) e^{-c_3 \Delta\tau_k} V|_{k-1}^+ \tag{28}$$

for any $\mathbf{x}(0^+) \in B_d(\mathbf{0})$, where $d = \min\{d_3, d_4\}$. If $\mathbf{K}_P$ and $\mathbf{K}_D$ are chosen such that

$$\tilde{L}\frac{c_2}{c_1}(2 + \varepsilon) e^{-c_3 \Delta\tau_k} < 1 \tag{29}$$

holds, then the sequence $\{V|_1^+, V|_2^+, V|_3^+, ...\}$ is strictly decreasing for any $\mathbf{x}(0^+) \in B_d(\mathbf{0})$.

Therefore, if the PD gains are chosen such that $\mathbf{A}$ in Eq. (14) is Hurwitz and that Eq. (29) is satisfied for any $\mathbf{x}(0^+) \in B_d(\mathbf{0})$, then the closed-loop hybrid time-varying system in Eq. (14) is locally exponentially stable. ■

VI. Simulation Results

In this section, dynamic walking of a 3-D bipedal robot with nine revolute joints (see Fig. 1) is simulated to evaluate the proposed control strategy. Physical parameters of the biped model in Fig. 1 are chosen as: $m_1 = 3$ (kg), $m_2 = 6$ (kg), $m_T = 20$ (kg); $l_1 = l_2 = \frac{l_3}{2} = 0.4$ (m), $w = 0.3$ (m).

A. Motion Planning

The desired trajectories for the biped to follow are determined by the desired contour, the desired position trajectory along the contour, and the desired walking pattern. Without loss of generality, the desired straight-line contour is chosen as the X_w-axis. Also, it is assumed that the desired position trajectory $s_d(t)$ is provided by a high-level planner and that $s_d(t)$ is monotonically increasing and continuously differentiable in t. Thus, the remaining task of motion planning is to plan the desired function $\boldsymbol{\phi}(\theta)$, which defines the desired walking pattern, such that necessary constraints and conditions are satisfied.

Similar to our previous study [20]–[22], optimization is utilized to find the desired function $\boldsymbol{\phi}(\theta)$. Besides the conditions (A1)–(A3) and $\phi_1, \phi_2, \phi_3 = 0$, feasibility constraints such as joint position limits and ground contact constraints are also considered in the optimization. The optimization variables are $\mathbf{a}_k$ ($k \in \{0, 1, ..., M\}$) as defined in Eq. (9).

B. Simulated Contouring Control of Fully Actuated 3-D Bipedal Robotic Walking

To illustrate the high versatility of the proposed walking strategy, a bipedal robot is commanded to track a straight-line contour (i.e., the X_w-axis) and a desirable position trajectory $s_d(t)$, which has an aperiodically varying velocity profile and is chosen as $s_d(t) = 2.3e^{-0.3(t+0.5)} + 0.6t - 2.2$ (m).

The PD gains $\mathbf{K}_P$ and $\mathbf{K}_D$ are chosen as: $\mathbf{K}_P = K_p \mathbf{I}_{9\times 9}$, $K_p = 841$; $\mathbf{K}_D = K_d \mathbf{I}_{9\times 9}$, $K_d = 58$. They yield a pair of real closed-loop poles at $p_{1,2} = -29$ (rad/s) for the continuous dynamics. Thus, $\mathbf{A}$ in Eq. (14) is Hurwitz.

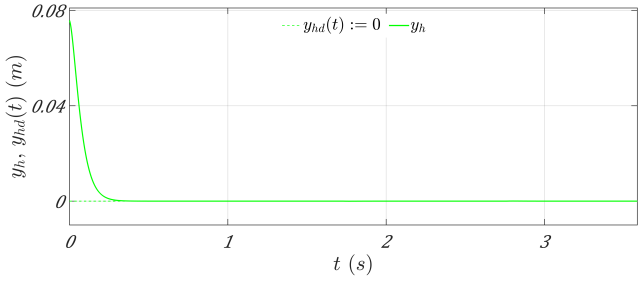

Fig. 2. Exponential tracking of the desired straight-line contour Γ_d. Desired contour Γ_d: X_w-axis. Desired position trajectory along Γ_d: $s_d(t) = 2.3e^{-0.3(t+0.5)} + 0.6t - 2.2$ (m).

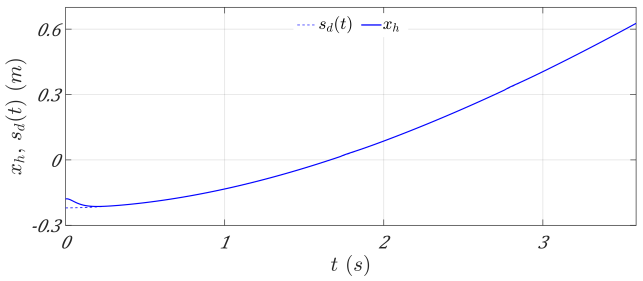

Fig. 3. Exponential tracking of the desired position trajectory $s_d(t)$ along the desired contour Γ_d. Desired contour Γ_d: X_w-axis. Desired position trajectory along Γ_d: $s_d(t) = 2.3e^{-0.3(t+0.5)} + 0.6t - 2.2$ (m).

As shown in Fig. 2, the biped's global position (i.e., (x_h, y_h)) exponentially converges to the desired contour (i.e., X_w-axis). Fig. 3 shows that the biped also exponentially follows the desired position trajectory $s_d(t)$ along the desired contour. These two figures clearly illustrate that the proposed walking strategy enables exponential contour tracking in 3-D Cartesian space for fully actuated bipedal robots, which has not been fully investigated in previous studies. In addition, Fig. 4 indicates that the biped's actual gait exponentially converges to the desired walking pattern.

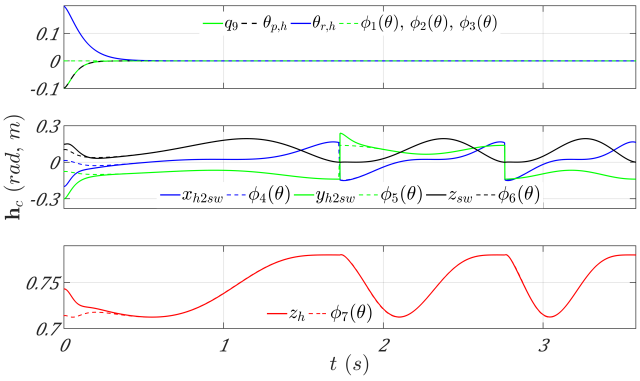

Fig. 4. Exponential tracking of the desired walking pattern $\mathbf{h}_c(\mathbf{q}) - \boldsymbol{\phi}(\theta(\mathbf{q})) = \mathbf{0}$. Desired contour Γ_d: X_w-axis. Desired position trajectory along Γ_d: $s_d(t) = 2.3e^{-0.3(t+0.5)} + 0.6t - 2.2$ (m).

VII. Conclusions

Based on state feedback control and formal stability analysis, this paper has proposed and developed a controller design that can realize exponential tracking of a straight-line contour for fully actuated 3-D bipedal robots. With the output function designed as the tracking errors of the desired straight-line contour, the desired motion along the contour, and the desired walking pattern, an input-output linearizing controller was synthesized to drive the output function exponentially to zero during continuous walking phases. By carefully selecting and encoding the desired walking pattern, conditional hybrid invariance was constructed for the desired motion. Sufficient closed-loop stability conditions were then established, and simulation results on a 9-DOF, 3-D biped validated the effectiveness of the proposed walking strategy in achieving high walking versatility for fully actuated 3-D bipedal robots. In future work, we will extend the proposed contouring control strategy from straight-contour to general-contour tracking as well as from fully actuated walking to multi-domain walking that consists of both fully actuated and underactuated walking.

References

[1] M. Vukobratović and B. Borovac, "Zero-moment point–thirty five years of its life," *Int. J. Humanoid Robot.*, vol. 1, no. 01, pp. 157–173, 2004.

[2] S. Kajita, F. Kanehiro, K. Kaneko, K. Fujiwara, K. Harada, K. Yokoi, and H. Hirukawa, "Biped walking pattern generation by using preview control of zero-moment point," in *Proc. IEEE Int. Conf. Robot. Autom.*, 2003, pp. 1620–1626.

[3] J. Grizzle, G. Abba, and P. Plestan, "Asymptotically stable walking for biped robots: Analysis via systems with impulse effects," *IEEE Trans. Autom. Contr.*, vol. 46, no. 1, pp. 51–64, 2001.

[4] E. R. Westervelt, J. W. Grizzle, and D. E. Koditschek, "Hybrid zero dynamics of planar biped walkers," *IEEE Trans. Autom. Control*, vol. 48, no. 1, pp. 42–56, 2003.

[5] B. Morris and J. W. Grizzle, "Hybrid invariant manifolds in systems with impulse effects with application to periodic locomotion in bipedal robots," *IEEE Trans. Autom. Contr.*, vol. 54, no. 8, pp. 1751–1764, 2009.

[6] B. G. Buss, A. Ramezani, K. A. Hamed, B. Griffin, K. S. Galloway, and J. W. e. a. Grizzle, "Preliminary walking experiments with underactuated 3d bipedal robot marlo," in *Proc. IEEE Int. Conf. Intell. Robot. Syst.*, 2014, pp. 2529–2536.

[7] X. Da, O. Harib, R. Hartley, B. Griffin, and J. W. Grizzle, "From 2D design of underactuated bipedal gaits to 3D implementation: Walking with speed tracking," *IEEE Access*, vol. 4, pp. 3469–3478, 2016.

[8] S. Kolathaya, A. Hereid, and A. D. Ames, "Time dependent control lyapunov functions and hybrid zero dynamics for stable robotic locomotion," in *Proc. American Contr. Conf.*, 2016, pp. 3916–3921.

[9] K. A. Hamed and J. W. Grizzle, "Event-based stabilization of periodic orbits for underactuated 3-D bipedal robots with left-right symmetry," *IEEE Transa. Robotics*, vol. 30, no. 2, pp. 365–381, 2014.

[10] A. D. Ames, E. A. Cousineau, and M. J. Powell, "Dynamically stable bipedal robotic walking with nao via human-inspired hybrid zero dynamics," in *Proc. ACM Int. Conf. Hybrid Syst.: Comput. Contr.*, 2012, pp. 135–144.

[11] A. D. Ames, "Human-inspired control of bipedal walking robots," *IEEE Trans. Autom. Contr.*, vol. 59, no. 5, pp. 1115–1130, 2014.

[12] A. D. Ames, P. Tabuada, A. Jones, W. L. Ma, M. Rungger, B. Schürmann, S. Kolathaya, and J. W. Grizzle, "First steps toward formal controller synthesis for bipedal robots with experimental implementation," *Nonlinear Analysis: Hybrid Systems*, 2017.

[13] C. Chevallereau, J. W. Grizzle, and C.-L. Shih, "Asymptotically stable walking of a five-link underactuated 3-D bipedal robot," *IEEE Trans. Robot.*, vol. 25, no. 1, pp. 37–50, 2009.

[14] C.-L. Shih, J. W. Grizzle, and C. Chevallereau, "From stable walking to steering of a 3D bipedal robot with passive point feet," *Robotica*, vol. 30, no. 07, pp. 1119–1130, 2012.

[15] H.-W. Park, A. Ramezani, and J. W. Grizzle, "A finite-state machine for accommodating unexpected large ground-height variations in bipedal robot walking," *IEEE Trans. Robot.*, vol. 29, no. 2, pp. 331–345, 2013.

[16] K. A. Hamed, B. G. Buss, and J. W. Grizzle, "Exponentially stabilizing continuous-time controllers for periodic orbits of hybrid systems: Application to bipedal locomotion with ground height variations," *Int. J. Robot. Res.*, vol. 35, no. 8, pp. 977–999, 2016.

[17] K. Sreenath, H.-W. Park, I. Poulakakis, and J. W. Grizzle, "A compliant hybrid zero dynamics controller for stable, efficient and fast bipedal walking on MABEL," *Int. J. of Robot. Res.*, vol. 30, no. 9, pp. 1170–1193, 2011.

[18] ——, "Embedding active force control within the compliant hybrid zero dynamics to achieve stable, fast running on MABEL," *Int. J. of Robot. Res.*, vol. 32, no. 3, pp. 324–345, 2013.

[19] T. Yang, E. R. Westervelt, and A. Serrani, "A framework for the control of stable aperiodic walking in underactuated planar bipeds," in *Proc. IEEE Int. Conf. Robot. Autom.*, 2007, pp. 4661–4666.

[20] Y. Gu, B. Yao, and C. S. G. Lee, "Time-dependent orbital stabilization of underactuated bipedal walking," in *Proc. American Contr. Conf.*, 2017, pp. 4858–4863.

[21] ——, "Bipedal gait recharacterization and walking encoding generalization for stable dynamic walking," in *Proc. IEEE Int. Conf. Robot. Autom.*, 2016, pp. 1788–1793.

[22] ——, "Exponential stabilization of fully actuated planar bipedal robotic walking with global position tracking capabilities," *J. Dyn. Syst. Meas. Control*, vol. 140, no. 5, p. 051008, 2018.

[23] C. Hu, B. Yao, and Q. Wang, "Global task coordinate frame-based contouring control of linear-motor-driven biaxial systems with accurate parameter estimations," *IEEE Trans. Ind. Electron.*, vol. 58, no. 11, pp. 5195–5205, 2011.

[24] B. Yao, C. Hu, and Q. Wang, "An orthogonal global task coordinate frame for contouring control of biaxial systems," *IEEE/ASME Trans. Mechatron.*, vol. 17, no. 4, pp. 622–634, 2012.

[25] H. K. Khalil, *Nonlinear control*. Prentice Hall, 1996.

[26] M. S. Branicky, "Multiple Lyapunov functions and other analysis tools for switched and hybrid systems," *IEEE Trans. Autom. Contr.*, vol. 43, no. 4, pp. 475–482, 1998.